Informes de la Construcción
Vol. 74, 568, e467
octubre-diciembre 2022
ISSN-L: 0020-0883
https://doi.org/10.3989/ic.91246

Simplified method for time-dependent effects in statically indeterminate concrete bridges with connected precast beams

Método simplificado para el cálculo diferido de puentes hiperestáticos de hormigón de vigas prefabricadas continuas

María Carmen Beteta (*), Luis Albajar (**), Carlos Zanuy (***), Miguel Estaún (****)

ABSTRACT

Nowadays, structural analysis programs are available to deal with continuous precast bridges with evolutive cross sections, but they hardly allow for a real control of the process with a full awareness of what consequences have the variation of the inputs in the final stress distribution. The present paper presents a simplified method as an improvement of the transformed section method with age-adjusted effective modulus for composite sections consisting of precast prestressed beams and a top concrete slab. The proposed method is verified by comparison with the comprehensive step-by-step method. The results are accurate not only in terms of stresses but also delayed curvatures, which allows its application, to all types of continuous bridges with staged construction process. The method is also applied to the calculation of a complex real bridge and the comparison of the results with the methods used in practice, as well as the criteria endorsed by experience.

Keywords*:* precast continuous bridges; aging coefficient; age-adjusted effective modulus; time-dependent stress redistribution.

RESUMEN

Actualmente existen programas de cálculo estructural para puentes prefabricados continuos con secciones evolutivas, pero difícilmente permiten un control real del proceso y de las consecuencias que tiene la variación de los datos de partida en la distribución final de tensiones. El presente trabajo presenta un método simplificado mejorado del método de la sección homogeneizada con un módulo efectivo ajustado a la edad para secciones compuestas constituidas por vigas prefabricadas pretensadas y una losa superior de hormigón. El método propuesto se verifica con el método paso a paso. Los resultados son precisos no solo en tensiones sino en curvaturas diferidas, lo que permite su aplicación, a todo tipo de puentes continuos con proceso constructivo evolutivo. Además, el método se aplica al cálculo de un puente real complejo y se comparan los resultados obtenidos con los métodos utilizados en la práctica, así como los criterios avalados por la experiencia.

Keywords: puentes prefabricados continuos; coeficiente de envejecimiento; módulo ajustado a la edad; redistribución de tensiones con el tiempo.

(*) MsC Civil Engineer. PhD Candidate, Universidad Politécnica de Madrid (U.P.M), Madrid (Spain).
(**) PhD Civil Engineer. Former Associate Professor, Dept. Continuum Mechanics and Structures (U.P.M), Madrid (Spain).
(***) PhD Civil Engineer. Associate Professor, Dept. Continuum Mechanics and Structures (U.P.M), Madrid (Spain).
(****) MsC Civil Engineer. Technical Director at STrucRes Engineering SL, specialized in the design of continuous precast bridges.
Persona de contacto/*Corresponding author*: maria.beteta@ineco.com (M.C. Beteta)
ORCID: http://orcid.org/0000-0001-9365-0624 (M.C. Beteta); http://orcid.org/0000-0002-2418-1921 (L. Albajar)
http://orcid.org/0000-0001-9044-8666 (C. Zanuy); http://orcid.org/0000-0002-9354-7368 (M. Estaún)

Cómo citar este artículo/*Citation:* Beteta, María Carmen; Albajar, Luis; Zanuy, Carlos; Estaún, Miguel (2022). Simplified method for time-dependent effects in statically indeterminate concrete bridges with connected precast beams. *Informes de la Construcción,* 74(568): e467. https://doi.org/10.3989/ic.91246

Recibido/*Received*: 20/09/2021
Aceptado/*Accepted*: 28/03/2022
Publicado on-line/*Published on-line*: 10/11/2022

1. INTRODUCTION

As in other countries, the construction of continuous bridges employing precast prestressed concrete girders began in the early 1990s in Spain as a step forward from the typology of single span bridges with precast U beams and a cast "in situ" slab (introduced in the 1980s). The connection between precast beams was initially achieved by means of a complementary external prestressing that provided compressive stresses in the joint, although the connection that finally prevailed consisted of local post-tensioned bars in the joint zone.

From the first applications, a complex design issue with constructive implications was the analysis of time-dependent stresses and deformations. The sequential or staged construction process generates changes in the structural shape, and delayed phenomena occur due to shrinkage and creep of the different concretes within the cross-section and the relaxation of the prestressing steel. These effects cause stress redistributions at the sectional level and change of internal forces at structural level (1-3).

In the late 1990s, due to the wider use of computational methods, extensive relevant experimental and numerical work was carried out by academics and designers (4-5). Among them, the developments by Prof. Marí's research group (6-10) were essential for the implementation of such methods in Spain. As a benchmark case, the Viaduct over Mente River, Figure 1, designed by Carlos Fernandez Casado SL was built in 1998 with length of 480m (spans of 2x30m+60m+3x90m+60m+30m). The cross section was 26,70 m wide and consisted of two precast U-shaped girders and a cast "in situ" slab. This technique, based on the connection between precast beams inside the span length, has been used for different types of bridges and is currently used in recent designs, Figure 2.

Figure 1. Viaduct over Mente River, Spain 1998.
(photo by the second author).

Though comprehensive finite element-based calculation methods including non-linearities have been progressively available for designers (e.g CONS software (11), developed by Prof. Marí) for the application to particular cases (12-15), the convenience of having simplified methods for the daily project was soon detected. Among them, the transformed section method with age-adjusted effective modulus (AAEM) based on the aging coefficient method by Trost and Bažant (16) has been the most widely used.

Figure 2. Viaduct in Villahermosa, Spain 2005
(photo by the fourth author).

The co-existence of complex calculation methods and approximate solutions has been maintained over time and currently both simplified and complex computational analyses are performed at different stages of the design. Moreover, the availability of experimental data from monitoring tools allows for refining the models. For example, the methodology used by Sousa et al. (17) on the Lezíria Bridge, has included a nonlinear finite element analysis calibrated with the experimental data obtained from monitoring and simplified methods (16) have been used for fitting shrinkage and creep functions for the concrete of the beam. In fact, the validity of simplified methods is still in force nowadays for "I" shaped beams with continuity by means of diaphragms on piers and with one stage of casting the slab in the cross section (18). This simplified method based on the aging coefficient calculates the indeterminate statically bending moment over piers considering gross sections, neglecting the reinforcement, and adding the prestressing losses afterwards.

As a relevant basis for simplified methods, the aging coefficient concept is based on the principle of linear superposition in time (19). The strain of a concrete member subjected to sustained stress, $\varepsilon_c(t)$, is proportional to the applied stress, $\sigma_c(t_o)$, (first term of Equation [1]). When the applied stress changes progressively with time, the total strain of concrete includes a second term as follows:

$$[1] \quad \boldsymbol{\varepsilon_c(t) = \sigma_c(t_0) \cdot \frac{1+\varphi(t,t_0)}{E_c(t_0)} + \int_{\tau=t_0}^{t} \frac{1+\varphi(t,\tau)}{E_c(\tau)} d\sigma_c(\tau)}$$

Where $\varphi(t, t_o)$ is the creep coefficient in the period (t, t_o) and $E(t_o)$ is the modulus of elasticity of concrete at age t_o. The integral term in Equation [1] can be solved by the aging coefficient $\chi(t, t_o)$, which allows deriving the time-dependent strain of concrete at any time t, and including shrinkage, $\varepsilon_{cs}(t, t_o)$, Equation [2] can be written as follows:

$$[2] \quad \boldsymbol{\varepsilon_c(t) = \sigma_c(t_0) \cdot \frac{1+\varphi(t,t_0)}{E_c(t_0)} + \frac{1+\chi(t,t_0)\cdot\varphi(t,t_0)}{E_c(t_0)} \Delta\sigma_c(t,t_0) + \varepsilon_{cs}(t,t_0)}$$

The linearity assumption is correct within the range of stresses in service conditions and allows for superposition of strains produced by stress increments (or decrements) and by shrinkage, Figure 3. The hypothesis of the aging coefficient model assumes that the aging coefficient χ has the same value for any process where strains are linear with the creep function (19) and stresses are proportional (actually, quasi-pro-

portional) to the relaxation function of concrete, $\xi(t, t_0)$, (16), refer to Figure 3. The constitutive model to describe the time-dependent concrete behavior with the aging coefficient provides a good approximation of the more complex step-by-step method for the study of partially restrained processes, such as those dealing with prestressing losses, stress redistribution of tall reinforced concrete piers, and staged construction of bridges.

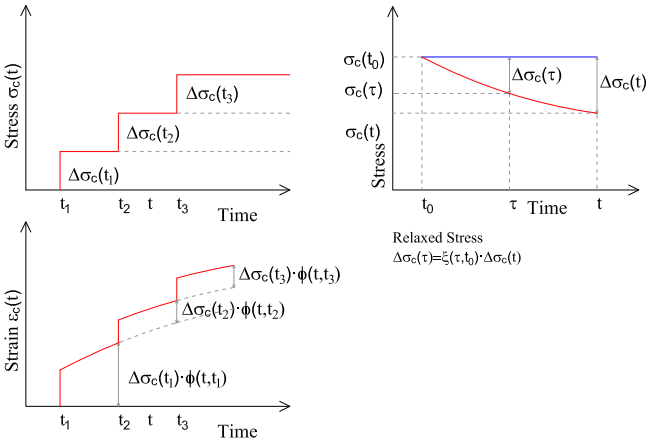

Figure 3. Step by Step Method versus Aging Coefficient Method.

As a reference mode for sectional analysis, the simplified method by Ghali et al. (16) (SMG hereafter) makes use of the transformed section method with AAEM to solve the time-dependent redistribution of stresses within composite sections by means of a sectional algorithm like the one used to solve the problem of a homogeneous section subjected to a nonlinear imposed deformation (for example, a nonlinear temperature gradient (20)). For the homogenization of the composite section, the aging coefficient by Trost and Bažant (19) is used for the constitutive behavior of concrete over time.

Despite the inherent advantages of the SMG, it presents some restrictions for the analysis of composite sections consisting of a prestressed beam and a cast "in situ" slab. The limitations of the method arise in the period after casting the slab (t_∞, t_1), where t_1 is the age of casting the slab and t_∞ is the end time (in addition, the age of prestressing of the beam will be referred to as t_0). The most important restrictions of the SMG are:

1) The fundamental hypothesis for the application of the aging coefficient model (quasi-proportionality of the stress process) is hardly fulfilled in the period after casting the slab (t_∞, t_1). This interval is studied by Ghali et al. (16) as a single stage with a combination of three stress sources for both concretes (creep originated by the initial loads, shrinkage of the beam and the slab, and stress redistributions over time due to the action of the slab weight from instant t_1).

2) The free creep strain of the beam in the period (t_∞, t_1) due to the variation of stresses in the beam in the period (t_1, t_0) –caused by shrinkage of the beam, creep due to self-weight of the beam and prestressing forces, and relaxation of the prestressing steel- is solved by transforming them into an instantaneous stress increase at an intermediate time t' within the interval (t_1, t_0).

3) The classic values of the aging coefficient χ are obtained from a process of relaxation (full restrain) of the concrete, different from the actual partial restrain and neglecting the shrinkage (despite it is a fundamental action of the slab).

Compared with the step-by-step method, the SMG provides good results in terms of stresses of the beam, but the values of delayed curvatures of the section in the period (t_∞, t_1) differ significantly according to the experience accumulated by precast companies from the 90s as it will be shown in the present paper, which in fact restricts the application of the SMG to statically determinate structures. Our new proposal includes dividing the whole process into process of quasi-proportional stresses, so that the aging coefficient can be applied consistently as a practical simplification of the step-by-step method.

In the present paper, an improved simplified methodology is presented to overcome the drawbacks of the SMG for composite sections consisting of precast prestressed beams and a top concrete slab built at a different time. The methodology is presented in Section 2 of the paper. The model introduces improvements to the SMG for composite sections to solve some of its conceptual inconsistencies that ultimately lead to an improvement of results, especially regarding delayed curvatures. Moreover, the model can be applied to the staged construction of continuous bridges consisting of precast beams with a cast "in situ" slab. In Section 3, the proposed method is verified by comparison with the step-by-step method. The results are accurate not only in terms of stresses but also regarding curvatures, including delayed ones, which allows its application, by integrating curvatures and using the flexibility nuance, to continuous bridges with staged construction process. In Section 4, the method is applied to the calculation of a complex real bridge and the comparison of the results with those obtained with the methods used in practice, as well as the criteria endorsed by experience.

2. PROPOSED METHOD FOR COMPOSITE SECTION ANALYSIS

A simplified method is proposed as an improvement of the SMG for composite sections consisting of a precast prestressed beam and a top reinforced concrete slab. The proposed improvement is considered useful for initial sizing stages, checking for bulk errors in input data when using complex software and, in general, as a definitive method of analysis.

2.1. Refined age-adjusting coefficient

A first authors' approach to a refined aging coefficient χ_{adj} that considers both the influence of shrinkage, and the restraining effect of the reinforcement was reported by Albajar et al (21). Such an idea was later improved by Fernandez Ruiz (22). The objective is to derive a value χ_{adj} from the analysis of a concrete prism with centrically embedded reinforcement. The concrete is first subjected to a compressive force, Figure 4.

Perfect bond is assumed between concrete and steel thus strains of concrete and steel must be equal. The reinforcement restrains the free time-dependent deformation of the concrete and a force variable with time develops in opposite direction to restore steel and concrete compatibility, Figure 4.

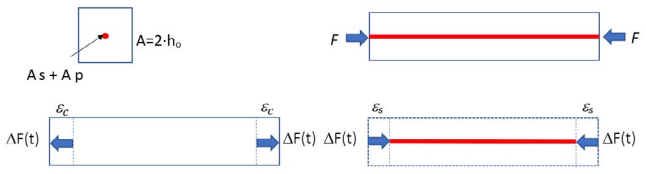

Figure 4. Tie model to calculate $c_{adj.}$

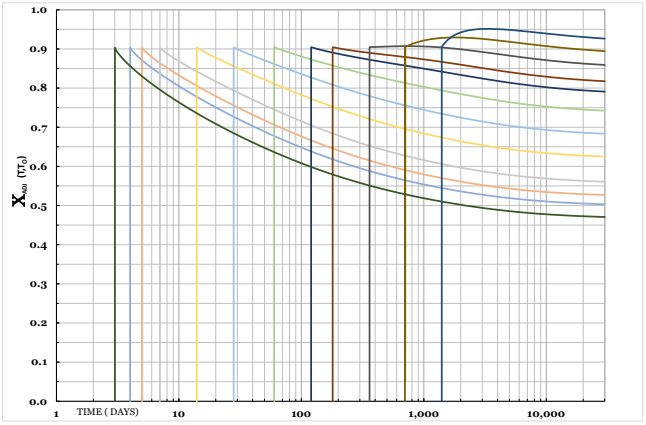

Figure 5. Adjusted Age coefficient of concrete c_{adj} (beam) fck=45MPa; RH=60%; ho=200mm; Ap=3%.

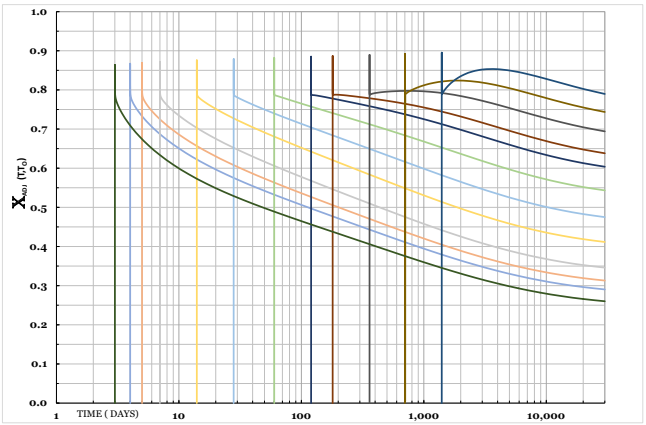

Figure 6. Adjusted Age coefficient of concrete c_{adj} (slab) fck=25MPa; RH=60%; ho=300mm.

The superposition principle is applied step by step. From the calculated stresses, the aging coefficient is obtained using its own definition. By varying the amount of reinforcement, the initial stress and the eventual concrete shrinkage, the coefficient χ_{adj} is obtained for different cases. The traditional value of χ can be derived from this approach as a particular case without shrinkage and with infinite reinforcement amount.

Figure 5 shows the values of χ_{adj} for h_o = 200 mm, fck = 45 MPa, RH = 60% and prestressing and reinforcement amount of 3% (parameters which correspond to the precast U-shaped beam studied later in this paper). Figure 6 shows the values of χ_{adj} for h_o = 300 mm, fck = 25MPa, RH=60% (parameters which correspond to the top slab studied later in this paper). As it is shown in Figure 6, the value of χ_{adj} for the slab is 0,26 which is less than the traditional value of χ for the slab with the same characteristics, 0,65.

2.2. Background to the SMG

The procedure of analysis of the time-dependent changes of strains and stresses in a non-cracked prestressed concrete section according to the SMG based on the transformed section with AAEM (16) is as follows (refer to Figure 7):

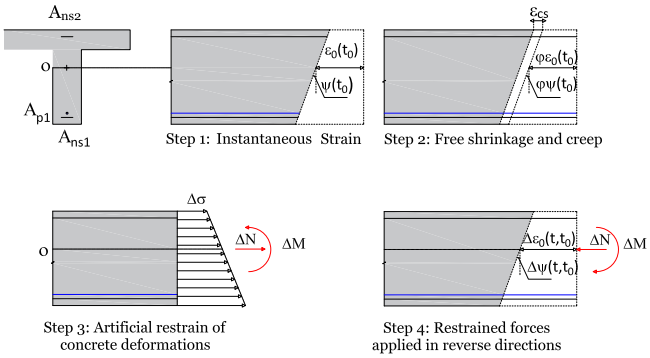

Figure 7. Steps of analysis of time-dependent strain and stress in a prestressed concrete section. Ghali et al. (16).

1) Determine the instantaneous strain due to the initial loads (self-weight and prestressing of the beam) with the use of the transformed section properties with instantaneous moduli for concrete and steel: axial strain at a reference point o $\varepsilon_o(t_o)$ and sectional curvature $\psi(t_o)$.

2) Determine the free strain distribution due to creep and shrinkage in the period from t_o to t. The strain change at the reference point $\varepsilon_o(t, t_o)$ and the change in curvature $\psi(t, t_o)$ in the period are:

$$[3] \quad \boldsymbol{\varepsilon_0(t,t_0) = \varepsilon_0(t_0)\cdot\varphi(t,t_0) + \varepsilon_{cs}(t,t_0)}$$

$$[4] \quad \boldsymbol{\psi(t,t_0) = \psi(t_0)\cdot\varphi(t,t_0)}$$

3) Calculate the artificial restraint stress on the concrete $\Delta\sigma_{rest}$ during the period from t_o to t to prevent the free strain calculated in step 2. Given the linear elastic behavior of the materials with the age-adjusted modulus for concrete, the stresses on the concrete can be calculated by multiplying the strain at any fiber by the age-adjusted modulus $E_c(t, t_o)$.

$$[5] \quad \boldsymbol{\Delta\sigma_{rest}(t,t_0) = -E_c(t,t_0)\cdot[\varphi(t,t_0)\cdot(\varepsilon_0(t_0) + \psi(t_0)\cdot y) + \varepsilon_{cs}(t,t_0)]}$$

The resultant of this stress can be represented by an axial force at o and a bending moment (restrained forces) as follows:

$$[6] \quad \boldsymbol{\Delta N_{rest}(t,t_0) = \int \Delta\sigma_{rest}(t,t_0)\, dA}$$

$$[7] \quad \boldsymbol{\Delta M_{rest}(t,t_0) = \int \Delta\sigma_{rest}(t,t_0)\cdot y\, dA}$$

4) The artificial restraint is released by the application of the forces ΔN_{rest} and ΔM_{rest} in opposite directions on the age-adjusted transformed section and the increment of axial strain $\Delta\varepsilon_o(t, t_o)$ and curvature $\Delta\psi(t, t_o)$ in the period are obtained.

5) Once the strain increment is known, the stress change on concrete is calculated multiplying the strain by the age-adjusted $E_c(t, t_o)$ modulus in the period (t, t_o). The stress increment of

the steel (prestressed and non-prestressed) is calculated multiplying the strain by its corresponding modulus of deformation.

6) At time t, the strain distribution is the sum of the strains obtained in steps 1 and 4, while the stress distribution is the sum of stresses of steps 1, 3 and 4.

In the case of composite sections, SMG (16) uses the same approach for the period (t_∞, t_1) including delayed effect of period (t_1, t_o) and the weight and shrinkage effect of the slab are considered together in the same process as indicated in the introduction.

2.3. Improved Simplified Method based on Aging Coefficient.

The proposed method is applied for composite sections consisting of a prestressed beam and a cast "in situ" slab. The method keeps the same methodology as the SMG up to the time of casting of the slab (instant t_1) but considering for the beam the value of χ_{adj} instead of χ. Thereafter, the method consists of dividing the effects of the slab in the period (t_∞, t_1) in two processes: process 1 that considers the effect of the slab shrinkage and process 2 that considers the effect of the creep due to the self-weight of the slab.

Thus, the long-term process is split in two stages which separately fulfill the condition of quasi-proportionality of stresses. Decomposition is consistently justified, and the application of the superposition principle is correct as there is no cracking under permanent loads. An overview of the two processes is sketched in Figure 8.

2.3.1. Process 1: shrinkage of the slab

This process considers the slab shrinkage and the restraining effect due to the fact that the slab prevents the beam from free shortening. The slab is considered without weight (considered in process 2). The refined aging coefficients χ_{adj} are applied for both the beam and the slab. Such aging coefficients χ_{adj} include the shrinkage of each concrete and the restraining effects due to the presence of the reinforcement of the beam and the monolithic interaction with the slab.

Relaxation of prestressing steel of precast beam is considered in this process. Reduced relaxation is obtained from intrinsic relaxation according to Ghali et al (16).

This process is solved with the following steps, refer to Figure 9:

1) Determine the strain and stress increment in the beam of the period (t_1, t_o). Axial deformation $\Delta\varepsilon_{ob}(t_1, t_o)$, curvature $\Delta\psi_b(t_1,t_o)$ and stress increment $\Delta\sigma_{cb}(t_1, t_o)$ of the beam are calculated according to the SMG described in Section 2.2 but with the values of χ_{adj} for the aged-adjusted modulus of concrete of the beam.

2) Determine the strain and stress increment of the beam of the period (t_∞, t_o) as if the slab had not been installed at t_1 due to self-weight and prestressing of the beam. Calculate axial deformation $\Delta\varepsilon_{ob}(t_\infty, t_o)$, curvature $\Delta\psi_b(t_\infty, t_o)$ and stress increment $\Delta\sigma_{cb}(t_\infty, t_o)$ of the beam.

3) Determine the strain and stress increment of the beam in the period (t_∞, t_1). Axial deformation $\Delta\varepsilon_{ob}(t_\infty, t_1)$, curvature $\Delta\psi_b(t_\infty, t_1)$ and stress increment $\Delta\sigma_{cb}(t_\infty, t_1)$ in the beam are calculated by difference from the values obtained in the periods (t_∞, t_o) and (t_1, t_o), steps 1 and 2, Figure 9.

$$[8]\quad \Delta\varepsilon_{0b}(t_\infty, t_1) = \Delta\varepsilon_{0b}(t_\infty, t_0) - \Delta\varepsilon_{0b}(t_1, t_0)$$

$$[9]\quad \Delta\boldsymbol{\psi}_b(\boldsymbol{t}_\infty, \boldsymbol{t}_1) = \Delta\boldsymbol{\psi}_b(\boldsymbol{t}_\infty, \boldsymbol{t}_0) - \Delta\boldsymbol{\psi}_b(\boldsymbol{t}_1, \boldsymbol{t}_0)$$

$$[10]\quad \Delta\boldsymbol{\sigma}_{cb}(\boldsymbol{t}_\infty, \boldsymbol{t}_1) = \Delta\boldsymbol{\sigma}_{cb}(\boldsymbol{t}_\infty, \boldsymbol{t}_0) - \Delta\boldsymbol{\sigma}_{cb}(\boldsymbol{t}_1, \boldsymbol{t}_0)$$

The former would be the strains and stresses developed in the beam in the period (t_∞, t_1) if there were no slab. The presence of the slab partially restrains the previous strains and creates additional self-equilibrated stresses, which are evaluated in the following steps.

4) The beam strain from the previous step $\Delta\varepsilon_{ob}(t_\infty, t_1)$ and $\Delta\psi_b(t_\infty, t_1)$ is restrained with the application of restraining forces in the beam $\Delta N_b(t_\infty, t_1)$ and $\Delta M_b(t_\infty, t_1)$, which can be calculated exactly:

$$[11]\quad \begin{pmatrix}\Delta\boldsymbol{N}_b(\boldsymbol{t}_\infty, \boldsymbol{t}_1)\\ \Delta\boldsymbol{M}_b(\boldsymbol{t}_\infty, \boldsymbol{t}_1)\end{pmatrix} = -\boldsymbol{E}_{cb}(\boldsymbol{t}_\infty, \boldsymbol{t}_1)\cdot\begin{bmatrix}\boldsymbol{A} & \boldsymbol{B}\\ \boldsymbol{B} & \boldsymbol{I}\end{bmatrix}\cdot\begin{pmatrix}\Delta\boldsymbol{\varepsilon}_{0b}(\boldsymbol{t}_\infty, \boldsymbol{t}_1)\\ \Delta\boldsymbol{\psi}_b(\boldsymbol{t}_\infty, \boldsymbol{t}_1)\end{pmatrix}$$

where $E_{cb}(t_\infty, t_1)$ is the aged-adjusted modulus of the beam concrete with the value of $\chi_{adj,b}$, as follows:

$$[12]\quad \boldsymbol{E}_{cb}(\boldsymbol{t}_\infty, \boldsymbol{t}_1) = \frac{\boldsymbol{E}_{cb}(\boldsymbol{t}_1)}{1+\boldsymbol{\chi}_{adj,b}(\boldsymbol{t}_\infty, \boldsymbol{t}_1)\cdot\boldsymbol{\varphi}_b(\boldsymbol{t}_\infty, \boldsymbol{t}_1)}$$

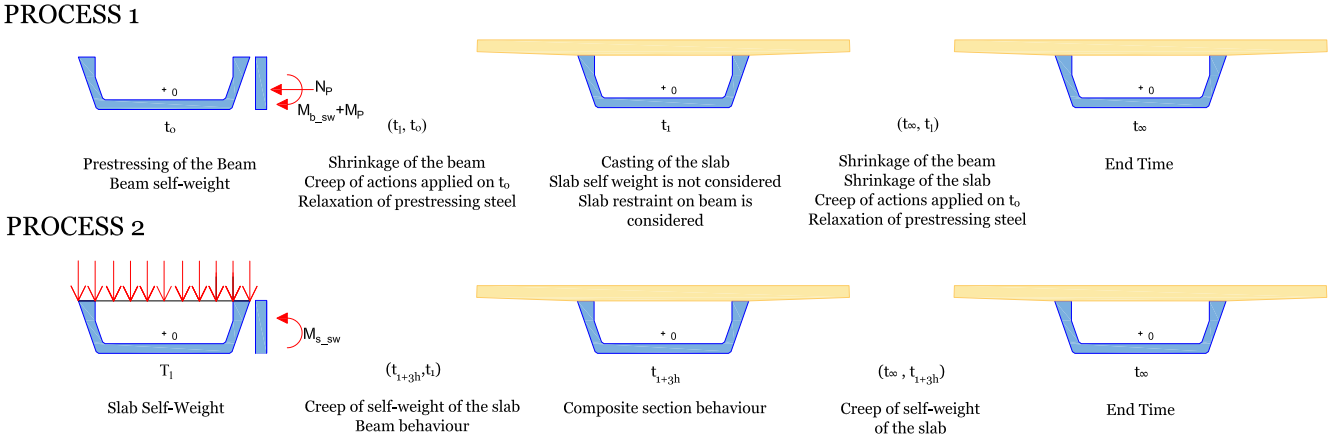

Figure 8. Description of the processes of the Improved Simplified Method.

where A, B and I are the area, first and second moment about, the axis through the reference point o of the age-adjusted transformed section of the beam in the period (t_∞, t_1).

5) Restrain of free strains of the slab. Restraining forces of the slab due its shrinkage ε_{cs} (t_∞, t_1) can be calculated as follows:

$$[13] \quad \begin{pmatrix} \Delta N_s(t_\infty, t_1) \\ \Delta M_s(t_\infty, t_1) \end{pmatrix} = -E_{cs}(t_\infty, t_1) \cdot \varepsilon_{cs}(t_\infty, t_1) \cdot \begin{bmatrix} A_{cs} \\ B_{cs} \end{bmatrix}$$

where E_{cs}(t_∞, t_1) is the aged-adjusted modulus of the concrete slab with the value of $\chi_{adj,s}$, Equation [14] and A_{cs}, B_{cs} are the area and first moment about, the axis through the reference point o of the concrete of the slab.

$$[14] \quad E_{cs}(t_\infty, t_1) = \frac{E_{cs}(t_1)}{1+\chi_{adj,s}(t_\infty, t_1) \cdot \varphi_s(t_\infty, t_1)}$$

6) Calculate the total restraining forces of the composite section ΔN_{comp} (t_∞, t_1) and ΔM_{comp} (t_∞, t_1) in the period (t_∞, t_1) as the sum of the restraining forces of the beam and the slab, calculated in steps 4 and 5, respectively.

$$[15] \quad \begin{pmatrix} \Delta N_{comp}(t_\infty, t_1) \\ \Delta M_{comp}(t_\infty, t_1) \end{pmatrix} = \begin{pmatrix} \Delta N_b(t_\infty, t_1) \\ \Delta M_b(t_\infty, t_1) \end{pmatrix} + \begin{pmatrix} \Delta N_s(t_\infty, t_1) \\ \Delta M_s(t_\infty, t_1) \end{pmatrix}$$

7) Apply the total restraining forces to the composite section in opposite direction. The increase of axial strain and curvature of the composite section $\Delta\varepsilon_{ocomp}$ (t_∞, t_1) and $\Delta\psi_{comp}$ (t_∞, t_1) in the time interval (t_∞, t_1) can be determined as:

$$[16] \quad \begin{pmatrix} \Delta\varepsilon_{0comp}(t_\infty, t_1) \\ \Delta\psi_{comp}(t_\infty, t_1) \end{pmatrix} = -\frac{1}{E_{cb}(t_\infty, t_1) \cdot (A_h \cdot I_h - B_h^2)} \cdot \begin{bmatrix} I_h & -B_h \\ -B_h & A_h \end{bmatrix} \cdot \begin{pmatrix} -\Delta N_{comp}(t_\infty, t_1) \\ -\Delta M_{comp}(t_\infty, t_1) \end{pmatrix}$$

where E_{cb} (t_∞, t_1) is the reference aged-adjusted modulus which corresponds to the beam concrete aged-adjusted modulus with the value of $\chi_{adj,b}$, and A_h, B_h and I_h are the area, first and second moment about the axis through the reference point o of the age-adjusted transformed section of the composite section in the period (t_∞, t_1).

8) To calculate the total effects of process 1, the stresses of the beam and the slab in the period (t_∞, t_1) are the sum of the restraining stresses plus the stresses obtained from the axial deformation and curvature of the composite section in the period (t_∞, t_1) given by step 7, while strains are those of step 7.

$$[17] \quad \Delta\sigma_{cs}(t_\infty, t_1) = \sigma_{rest_s}(t_\infty, t_1) + E_{cs}(t_\infty, t_1) \cdot (\Delta\varepsilon_{0comp}(t_\infty, t_1) + \Delta\psi_{comp}(t_\infty, t_1) \cdot y)$$

$$[18] \quad \Delta\sigma_{cb}(t_\infty, t_1) = \sigma_{rest_b}(t_\infty, t_1) + E_{cb}(t_\infty, t_1) \cdot (\Delta\varepsilon_{0comp}(t_\infty, t_1) + \Delta\psi_{comp}(t_\infty, t_1) \cdot y)$$

$$[19] \quad \sigma_{rest_s}(t_\infty, t_1) = -E_{cs}(t_\infty, t_1) \cdot \varepsilon_{cs}(t_\infty, t_1)$$

$$[20] \quad \sigma_{rest_b}(t_\infty, t_1) = \Delta\sigma_{cb}(t_\infty, t_1) - Ecb(t_\infty, t_1) \cdot (\Delta\varepsilon_{0b}(t_\infty, t_1) + \Delta\psi_b(t_\infty, t_1) \cdot y)$$

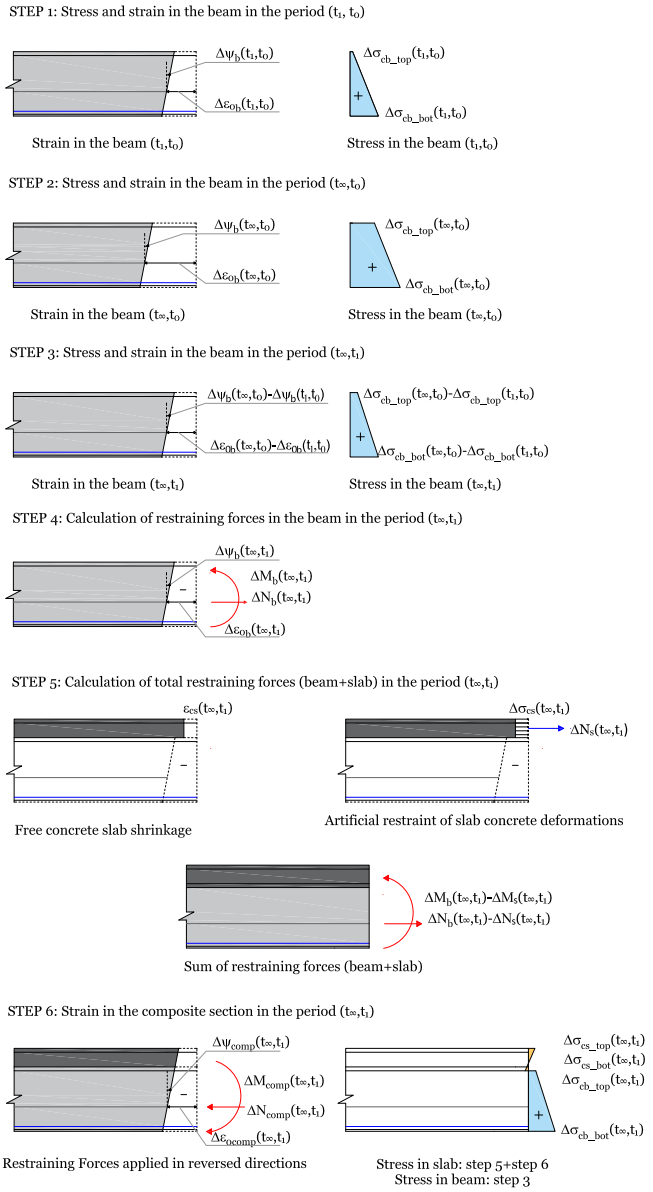

Figure 9. Steps of process 1. Proposed Improved Simplified Method.

9) The stress increment of the prestressing steel in the period (t_∞, t_1) in process 1 is calculated multiplying the strain obtained from the axial deformation and curvature of the composite section in the period (t_∞, t_1), step 6, by its corresponding modulus of deformation plus the stress decrement due to relaxation of prestressing steel in that period.

10) The stress increment of the non-prestressing steel in the period (t_∞, t_1) in process 1 is calculated multiplying the strain obtained from the axial deformation and curvature of the composite section in the period (t_∞, t_1), step 6, by its corresponding modulus of deformation.

2.3.2. Process 2: self-weight of the slab

This process starts at the instant of the casting of the slab at t_1 and ends at t_∞. An intermediate period of 3 hours is here introduced to separate the beam behavior from the composite monolithic behavior. The soft slab initially acts as a load on the beam, which is maintained for 3 hours (the time of 3 hours depends on the type of concrete and it has been adjust-

ed by applying a step-by-step analysis). Creep on the beam is considered in these three hours. Thereafter, the slab restrains the creep of the beam due to the load at t1 and the behavior becomes monolithic. The SMG (described in section 2.2) can be applied because the evolution of stresses in both concretes is quasi-proportional to the relaxation functions of the two concretes. However, the following improvements have been introduced with respect to the SMG methodology:

1) An intermediate stage of 3 hours is introduced between the casting of the slab and the monolithic behavior of the composite section to improve the results in terms of curvatures.

2) As there is no shrinkage (already included in process 1), the conventional value of the aging coefficient is used for both concretes with the corresponding ages but considering the reinforcement of the beam and the restraint of the slab.

The proposed method can be extended to the common practice of casting the slab in two phases: first stage casting the core of the section and second phase casting cantilevers.

2.4. Summary of improvements with respect to SMG

Splitting the long-term process into two processes in the period (t_∞, t_1) after casting the slab solves some issues which are not typically considered: 1) free creep strain of the beam in the period (t_∞, t_1) caused by the stresses developed in the previous period (t_1,t_0) and 2) the application of the aging model in a joint process considering simultaneously shrinkage of both concretes (beam and slab) and the creep of the beam due to the initial loads applied at t_0, including the prestressing and the weight of the slab acting from t_1. The restraining forces of the beam in the period (t_∞, t_1) are calculated exactly from the difference of strain values between (t_∞, t_0) and (t_1, t_0).

From the point of view of the concrete behavior, the following improvements have been achieved with respect to the traditional aging coefficient χ. For the beam, a refined χ_{adj} is used in all cases, which is calculated in a process of simultaneous creep and shrinkage and with the amount of restraining reinforcement corresponding to the total areas of prestressing and non-prestressing steel. For the cast "in situ" slab, the effect of shrinkage restrained by the beam predominates. The value of χ_{adj} is calculated for a fully constrained very low initial stress-free creep and shrinkage process.

3. COMPARISON OF THE PROPOSED MODEL WITH STEP-BY-STEP ANALYSIS OF A STATICALLY DETERMINATE BRIDGE.

3.1. Overview of studied case

The capabilities of the proposed method are studied by a comparison with a step-by-step analysis carried out with a software developed by Prof. Marí (23). In the step-by-step method, the total studied time is divided into short time intervals (steps) in which the constitutive behavior of the materials affected by time-dependent creep and shrinkage is restrained by the compatibility condition that plain sections remain plane. The section is divided into layers of concrete or steel, which are subjected to restraining stresses. Equilibrium of axial force and bending moment is imposed to achieve the unknown strain distribution of the section within each step.

The midspan cross-section of a simply supported bridge structure has been considered to study stresses, strains, and curvatures with the following three methods: the proposed model, the step-by-step analysis, and the SMG. The analyzed cross section is a precast pretensioned U-shaped beam with a depth of 1,60 m and a cast "in situ" slab of 4,80 m width and 0,30 m thickness. Both prestressing, A_{psi}, and non-prestressing steel A_{nsi}, are shown in Figure 10. The area and second moment about, the axis through the reference point 0 of the precast beam are A =1,040m^2 and I_0=0,342m^4.

The ages of the precast beam at the time of prestress and at the casting of the deck slab are 4 and 29 days, respectively. The prestressing force in the analyzed section is P=17702 kN after instantaneous losses, the bending moment due to the self-weight of the beam is M_{swbeam}= 3760 mKN and the bending moment due to the self-weight of the slab is M_{swslab}= 5490 mKN. The characteristic compressive strengths of concrete at 28 days are f_{ckbeam}= 45 MPa and f_{ckslab}= 25 MPa for the beam and the slab, respectively.

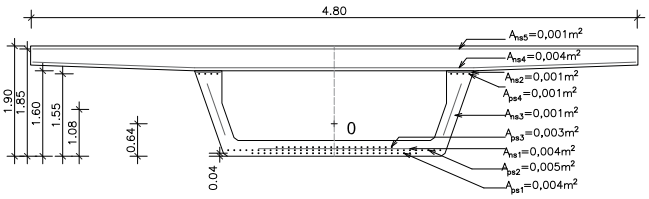

Figure 10. Studied cross section. Dimensions in m.

For the evaluation of rheological effects, the formulations of CEB-FIB Model Code (24) are used for shrinkage and creep of both concretes, relaxation of the prestressing steel and the time-dependent functions for both concretes' modulus of elasticity. Other input data are: Relative Humidity HR=60%, rapidly hardening high-strength cement for the concrete of the beam and normal hardening cement for the concrete of the slab. Low relaxation strands are considered.

Two analyses have been completed with the step-by-step method: (a) neglecting the weight of the slab to assimilate it to process 1, and (b) considering the weight of the slab, being this process the sum of processes 1 and 2. Results of process 2 with the step-by-step method are obtained by difference between the complete process and process 1 (without weight of the slab).

3.2. Results and conclusions

The results are shown in Table 1 and 2. Table 1 compares curvatures in each period with the three methods studied: SMG, step-by-step analysis, and the proposed method. It is important to point out that the values of instantaneous curvatures are the same with the three methods. The comparison focuses firstly on delayed curvatures in the period (t_∞, t_1) because they are relevant to obtain the redundant moments in continuous structures. Splitting the analysis into two processes gives accurate results in terms of delayed curvatures in the period from casting of the slab t_1 to end time t_∞ when they are compared with the step-by-step calculation. Differences between the step-by-step method and the proposed method are less than 1%.

Comparing the final stresses at age t_∞ at the bottom of the beam (which is the relevant point for crack control) obtained with the proposed model and the step-by-step method, the values are rather similar, with differences less than 1%. At the top of the beam, the differences between both methods are 5%. Regarding stresses of the slab, differences are 5% at the top, with no conclusive results at the bottom due to the low magnitude of the stresses at this fiber.

If the results from the SMG are compared with the step-by-step method, good agreement is obtained regarding stresses at the bottom of the beam (less than 5%) but the difference in delayed curvatures is significant. Therefore, the accuracy gained with the proposed model is demonstrated.

Table 1. Comparison of curvatures, ψ, between three methods.

Curvature ψ	t_o	(t_1, t_o)	t_1	(t_∞, t_o)
Proposed Method. Process 1. (m-1)	3,02E-04	-1,64E-04	-	-2,40E-04
Step-by-Step Method. Process 1 (m-1)	-3,02E-04	-1,77E-04	-	-2,39E-04
Proposed Method/ Step by Step (Process 1) (%)	1,00	0,93	-	1,00
Proposed Method. Process 2 (m-1)	-	-	3,93E-04	2,50E-04
Step-by-Step Method. Process 2 (m-1)	-	-	3,91E-04	2,48E-04
Proposed Method/ Step by Step (Process 2) (%)			1,00	1,01
SMG	-3,02E-04	-1,61E-04	3,93E-04	1,05E-06
Step-by-Step Method	-3,02E-04	-1,77E-04	3,91E-04	8,49E-06
SMG / Step-by-Step (%)	1,00	0,91	1,00	0,12

4. CASE-STUDY OF A STATICALLY INDETERMINATE BRIDGE: PROJECT FOR A VIADUCT OVER ABION RIVER.

4.1. Description of the Viaduct

A study is presented here taking as a basis a design project for a viaduct over the Abión River in Spain as a part of the Duero Highway Construction Project. The structure is 250 m long and is made up of six spans: 25,00 m + 40,00 m + 3x50,00 m + 35,00 m, Figure 11. The studied project corresponds to the widening of the left road.

The structure is continuous. The type of deck is a spliced U-shape precast post-tensioned girder with variable depth and a cast "in situ" concrete top slab using free standing planks. Cross section of the viaduct is shown in Figure 12.

Three types of precast beams are considered in the design: 1) Lateral beams which are in the extreme spans of the deck and are 28,00 m long. 2) Pier segment beams which are on the central piers of the structure and are 15,00m long and 3) Central beams which rest on pier segment beams and are 35,00 m long, except for beam 2, which is 30,0 m long. Continuity between precast beams is achieved by means of short straight tendons (BSST system). The top slab is post-tensioned at pier sections to avoid cracking and excessive deflections. Connection between beams is carried out by local prestressing unbonded bars, crossing through a wet joint poured with a high strength mortar. At the end of the spliced U-girders diaphragms with a shear key are defined Figure 13.

4.2. Description of the construction process

The constructive process considered in the project for the Abión River Viaduct consists of the following phases:

Phase 1: Construction of foundations, piers and abutments, placement of temporary supports, erection of pier segment beams and lateral beam nº1.

Phase 2: Erection of central beams and lateral beam nº10. Erection of free stranding planks. Pouring of high strength grout in the joint and post-tensioning of unbonded bars and placement of concrete.

Phase 3: Casting of the top slab, first stage: in longitudinal direction, casting 1/5 of the length of the span and in the transverse direction only the core without lateral cantilevers.

Table 2. Comparison of stresses between three methods.

STRESSES (MPa)	t_o			t_1			t_∞			%	
	SMG	Proposed Method	Step-by- Step Method	SMG	Proposed Method	Step-by- Step Method	SMG	Proposed Method	Step-by- Step Method	SMG / Step-by- Step Method	Proposed Method/ Step-by- Step Method
$\sigma_{ctopslab}$	0,00	0,00	0,00	0,00	0,00	0,00	-1,29	-0,99	-0,95	1,35	1,04
$\sigma_{cbotslab}$	0,00	0,00	0,00	0,00	0,00	0,00	-1,28	-1,48	-1,14	1,13	1,30
$\sigma_{ctopbeam}$	-6,64	-6,64	-6,63	-21,12	-21,12	-21,00	-10,37	-10,63	-11,14	0,93	0,95
$\sigma_{cbotbeam}$	21,38	-21,38	-21,38	-9,20	-9,18	-9,47	-8,18	-7,86	-7,89	1,04	1,00

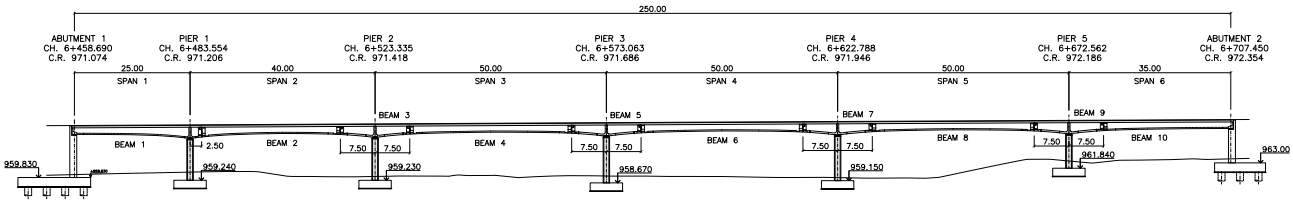

Figure 11. Elevation of Viaduct over Abión River.

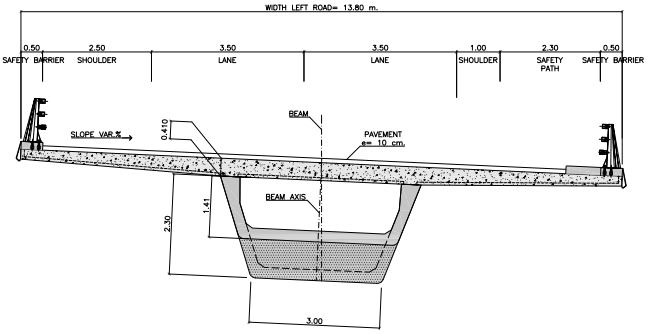

Figure 12. Cross section of Viaduct over Abión River.

Phase 4: Release of temporary supports and first phase of post-tensioning of the slab.

Phase 5: Erection of the rest of concrete planks.

Phase 6: Casting of the top slab, second stage: casting is completed in the remaining 3/5 length of the span length in longitudinal direction and in the transverse direction only the core without lateral cantilevers.

Phase 7: Second phase of post-tensioning of the slab.

Phase 8: Casting of the top slab, third stage: casting of lateral cantilevers.

Figure 13. Typical connection detail between beams.

4.3. Description of the calculation model

The construction sequence implies that two types of analysis must be carried out for the different loads involved: instantaneous loads and time-dependent effects.

For the analysis of the structure due to instantaneous loads, a calculation model with beam-type elements has been carried out using commercial Statik program (25). Statik is a finite element software for the linear-elastic analysis of three-dimensional frame structures according to the theories of first and second order. In this particular case, a linear first order analysis has been carried out for the instantaneous loads.

The bridge structure has been divided into 159 beam elements with a maximum length of 2.0 m. Thirty-four cross sections are defined based on the variable depth of the beam. Within each cross section, different types of variants of cross sections are defined: beam, composite section without cantilevers, and complete composite section depending on the construction process. Besides, each set of variants of cross-section considers different values of modulus of elasticity of the concrete depending on the ages of the beam and the slab at each phase. Load cases and post-tensioning cables are introduced in the calculation model according to the construction stages with the corresponding variant of cross section. Self-weight of precast planks is included in the self-weight of the slab as a simplification. The aim of the model is to obtain the instantaneous forces in the different sections of the Viaduct at each time instant, t_i, for each load case.

To carry out the time-dependent analysis and the redistribution of stresses in the cross-sections, the model proposed in the present paper is implemented into self-made spreadsheets. Each span is divided into five sections: extreme sections, L/4, midspan and 3L/4, where L is the length of the span. Each section is studied individually following the methodology described in section 2.3. The long-term process is split in two stages: process 1 that considers slab shrinkage and the self-weight and post-tensioning of the beam and process 2 that considers the self-weight and the post-tensioning of the slab, thereby focusing on creep phenomena. The second process considers the different phases of casting and post-tensioning of the slab.

Process 1 starts at t_o when post-tensioning of the beam - age of the beam considered is 10 days - has an intermediate instant t_2 or t_4 (depending on the moment of casting the slab: t_2 for sections over piers and t_4 for midspan section) and ends at t_∞. Casting of the slab is considered in a single phase as a simplification to study the slab shrinkage phenomenon. The steps and the formulae are those indicated in Section 2.3.1.

Process 2 starts at t_1 when the connection between beams is achieved and ends at t_∞. It has the following steps:

1) t_1: connection between beams. Self-weight of the central piers in pier segment beams. Age of beam is 21 days.

2) (t_1, t_0): creep due to the self-weight of the central beams in pier segment beams.

3) t_2: self-weight of the slab core due to the first stage of slab casting. Age of beam is 28 days and age of slab is 3 days.

4) (t_{2+3h}, t_2): creep in the defined period due to actions applied on the instants t_1 and t_2 acting on the beam.

5) (t_3, t_{2+3h}): creep in the defined period due to actions applied in the instants t_1 and t_2 acting on the composite section without lateral cantilevers.

6) t_3: withdrawal of temporary supports and first phase of post-tensioning of the slab. Age of beam is 35 days and age of slab is 10 days.

7) (t_4, t_3): creep in the defined period due to actions applied in each instant from t_1 to t_3 and relaxation of the slab prestressing strands. These actions are applied in the composite section without lateral cantilevers.

8) t_4: self-weight of the slab core corresponding to the second stage of slab casting. Age of beam is 37 days and age of slab is 12 days.

9) (t_5, t_4): creep in the defined period due to actions applied in each instant from t_1 to t_4 and relaxation of the slab prestressing strands. These actions are applied in the composite section without lateral cantilevers.

10) t_5: second phase of post-tensioning of the slab. Age of beam 44 days and age of slab 19 days.

11) (t_6, t_5): creep in the defined period due to actions applied in each instant from t_1 to t_5 and relaxation of the slab prestressing strands. These actions are applied in the composite section without lateral cantilevers.

12) t_6: self-weight of the cantilevers corresponding to the third stage. Age of beam 46 days and age of slab 21 days.

13) (t_{6+3h}, t_6): creep in the defined period due to actions applied in each instant from t_1 to t_6 and relaxation of the slab prestressing strands. These actions are applied in the composite section without lateral cantilevers.

14) (t_∞, t_{6+3h}): creep in the defined period due to actions applied in each instant from t_1 to t_6 and relaxation of the slab prestressing strands. These actions are applied in the complete composite section.

The evolution of strains and stresses in the slab and the beam and curvatures have been calculated for each step. The redistribution of stresses is determined at each studied section applying the proposed simplified model.

The redistribution of internal forces at structural level and the statically indeterminate bending moments are determined from delayed curvatures at each relevant time. The statically indeterminate bending moments due to dead loads including prestressing are evaluated indirectly from the Displacement Method. Delayed curvatures obtained in each section individually as an action that produces a deformation incompatible with the real structure, so the program calculates the redundant bending moments at supports that are needed to establish the compatibility of deformations.

Statik software has been used for the calculation of the statically indeterminate bending moments and six different models have been carried out depending on the type of the structure due to the construction process. Thus, two calculation models are considered for delayed curvatures in the periods (t_2, t_1) and (t_∞, t_2) for process 1 and four calculation models are carried out for delayed curvatures in the periods: (t_{2+3h}, t_1); (t_{4+3h}, t_{2+3h}); (t_{6+3h}, t_{4+3h}) and (t_∞, t_{6+3h}) for process 2. . Once the statically indeterminate bending moments are known, stresses caused by them are added at each relevant period for each section.

5. RESULTS

Stresses at the most critical sections are calculated as the sum of those due to self-weight, prestressing (beam and slab), statically indeterminate bending moments in the different intervals of time plus rheological phenomena. Results are shown in Figure 14. All sections are under compression except at the top of the slab at end supports, with a tensile stress of 1 MPa (lower than the tensile strength of the concrete of the slab). Such sections are assembled without prestressing.

Figure 14. Stresses (MPa) due to self-weight, prestressing, rheological effects, and statically indeterminate bending moment.

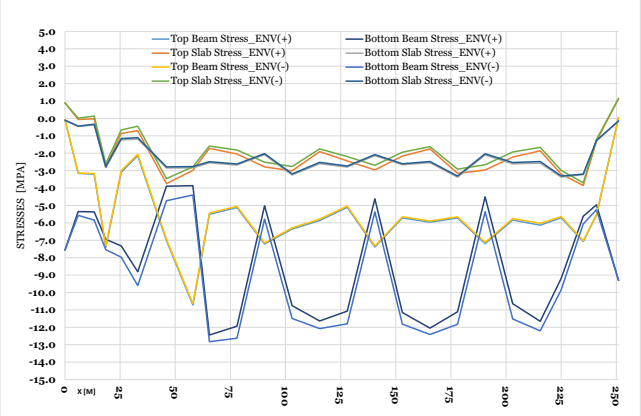

Figure 15. Stresses t_∞ (MPa). Quasi-permanent combination of loads.

Stresses under the quasi-permanent combination of loads at t∞ are shown in Figure 15 There are not tensile stresses in any concrete section. Maximum compressions are less than 60% of the compressive strength. All sections are under compressive stresses except at the top of the slab at end supports, with tensile stresses of 1 MPa (lower than the tensile strength of the concrete of the slab). Such sections are assembled without prestressing.

Stresses under the frequent combination of loads at t_∞ are shown in Figure 16 The maximum compression is less than 60% of the compressive strength of the beam (30MPa). At support sections, the top of the slab is compressed except for pier 1, where the tensile stress is 0,43 MPa. At midspan sections of spans 2, 3, 4 and 5, the bottom of the beam has tensile stress, being the maximum of 2MPa, so crack control checks have been carried in these sections. In addition, the crack control leads to crack widths smaller than 0,2 mm in frequent loads combination, assuming that the section is cracked under the characteristic combination.

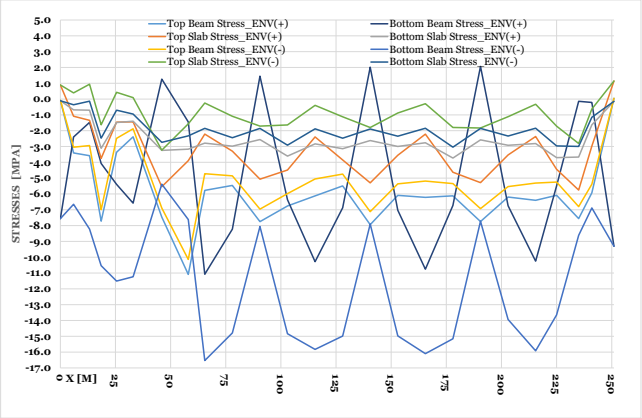

Figure 16. Stresses t∞ (MPa). Frequent combination of loads.

6. CONCLUSIONS

The present paper presents an improved simplified method based on the aging coefficient as an improvement of the SMG for composite sections consisting of precast prestressed beams and a top concrete slab built at a different time.

The improvements of the simplified method with respect to the SMG basically consist of splitting the long-term process into two processes in the period (t_∞, t_1) after casting the slab which separately fulfill the condition of quasi-proportionality of stresses: process 1 that considers the effect of shrinkage of the slab and the self-weight and prestressing of the beam and process 2 that considers the effect of creep due to the self- weight of the slab. This method also improves the value of the traditional aging coefficient defining a refined age-adjusted coefficient χ_{adj} which considers the effect of shrinkage and the amount of restraining reinforcement corresponding to the total areas of prestressing and non-prestressing steel in the case of the beam and a fully constrained very low initial stress-free creep in the case of the slab.

The method has been checked with a step-by-step model obtaining good results in terms of stresses and delayed curvatures. The SMG method provides good agreement regarding stresses in the beam but the difference in delayed curvatures is significant which limits its application to statically indeterminate concrete structures. Delayed curvatures in the period (t_∞, t_1) are a relevant result to obtain the redundant moments in continuous structures.

The method presented in this paper, and its suitability to be programmed even with spread sheets, can provide to the designers an alternative and quick method for the analysis, or just an easy way to check the results of our program calculations. As it has been checked with the calculations carried out with the proposed simplified method, the results obtained by this parallel analysis for the project of the left carriageway of Rio Abión Viaduct are quite like those used for the design checking. To enable this comparison, it has been carefully followed that the input data were the same than used for the design, and before reviewing the results it has been analyzed the similarity of the stresses in some of the multiple construction stages.

In conclusion, this simplified method provides enough accurate results to be used as a design tool for staged construction concrete bridges, without needing complex structural analysis programs to analyze time dependent effects of shrinkage and creep along the bridge, considering the different construction stages, the evolution in time of sections shapes and stiffness, and even the variation of boundary conditions.

ACKNOWLEDGEMENT

We thank Professor Antonio Marí Bernat. This paper expresses solely the opinion of the authors and does not imply any compromise for their institutions or third parties.

REFERENCES

(1) Collins, M.P.; Mitchell, D. (1997). *Prestressed Concrete Structures*. Canada: Response Publications.
(2) Gilbert, R.I.; Mickleborough, N.C. (1990). *Design of Prestressed Concrete*. Spon Press.
(3) Menn, C. (1990). *Prestressed Concrete Bridges*. Basel: Birkhäuser Verlag AG.
(4) Fédération Internationale du Béton (FIB) (2004). *Precast Concrete Bridges*. Bulletin 29. https://doi.org/10.35789/fib.BULL.0029
(5) Burón, M.; Fernández-Ordoñez, D.; Peláez, M. (1997). Prefabricación de puentes con tableros de losa pretensada continua. Realizaciones. *Hormigón y Acero*, 204, 77-83.
(6) Valdés López, M.; Marí Bernat, A.R.; Valero López, I.; Montaner Fragüet, J. (1998). Estudio experimental de un puente continuo de hormigón prefabricado. *Hormigón y Acero* 207, 21-34.
(7) Valdés López, M. (1997). *Comportamiento durante construcción y bajo cargas permanentes de puentes prefabricados de hormigón*. (PhD Thesis). Escuela Técnica Superior de Ingenieros de Caminos, Canales y Puertos, Barcelona, Spain.
(8) Cruz, P.J.S. (1995). *Un modelo para el análisis no lineal y diferido de estructuras de hormigón y acero construidas evolutivamente*. (PhD Thesis). Escuela Técnica Superior de Ingenieros de Caminos, Canales y Puertos, Barcelona, Spain.

(9) Marí, A.; Montaner, J.M.; Valdés, M. (1996). Investigación teórica y experimental sobre el comportamiento de estructuras de hormigón pretensado construidas evolutivamente. *XV Asamblea de la Asociación Técnica Española del Pretensado*. (Congreso de puentes y estructuras, Spain).
(10) Marí, A.; Valdés, M.; Cruz, P.J; Montaner, J.M. (1997). Continuous Precast Concrete Bridges Analysis and Experimental Evaluation. *International Conference New Technologies in Structural Engineering*, Lisbon, Portugal.
(11) Marí, A. (1984). Nonlinear geometric, material and time dependent analysis of three dimensional reinforced and prestressed concrete frames. *Report no UCB/SESM-84/12*, University of Berkeley, California.
(12) Pérez, G.A; Marí Bernat, A.R.; Danesi, R.F. (1999). Estudio experimental y numérico del comportamiento de puentes prefabricados monoviga bajo cargas de servicio. *Hormigón y Acero*, 211, 97-108.
(13) Pérez, G.A. (2000). *Estudio experimental y numérico del comportamiento en servicio y en rotura de puentes prefabricados monoviga.* (PhD Thesis). Escuela Técnica Superior de Ingenieros de Caminos, Canales y Puertos, Barcelona, Spain.
(14) Marí, A.; Montaner, J.M. (2000). Continuous Precast Concrete Girder and Slab Bridge Decks. Proceedings of the Institution of Civil Engineers. *Structures and buildings*, 140, 195-207. https://doi.org/10.1680/stbu.2000.140.3.195.
(15) Marí, A.; Valdés, M. (2000). Long-Term Behaviour of Continuous Precast Concrete Girder Bridge Model. *Journal of Bridge Engineering*, 5(1), 22-30. https://doi.org/10.1061/(ASCE)1084-0702(2000)5:1(22)
(16) Ghali, A.; Favre, R.; and Elbadry, M. (2019). *Concrete structures: Stresses and Deformations*. (4th ed) Spon London.
(17) Sousa, C.; Sousa, H.; Serra Neves, A.; Figueiras J. (2012). Numerical Evaluation of the long-term Behaviour of precast Continuous Bridge Decks. *Journal of Bridge Engineering*, 17(1), 89-96. https://doi.org/10.1061/(ASCE)BE.1943-5592.0000233
(18) Fédération Internationale du Béton (FIB) (2020). *Precast concrete bridge continuity over piers*, Technical report. Task Group 6.5 Bulletin 94. https://doi.org/10.35789/fib.BULL.0094.
(19) Bažant, Z.P. (1972). Prediction of concrete creep effects using age-adjusted effective modulus method. *ACI Journal*, 69, 212-217.
(20) de la Fuente Martín, P.; Zanuy Sánchez, C. (2017). Fundamentos para el cálculo de estructuras prismáticas planas. *Monografía del Instituto Torroja* Nº 424.
(21) Albajar Molera, L.; Lleyda Dionis, J.L. (1991). Ensayos de acortamiento para traviesas de desvío, *International Symposium on Precast Concrete Railway Sleepers*, 143-156. Madrid, Spain.
(22) Fernández Ruiz, M. (2004). Aplicación del método del coeficiente de envejecimiento a problemas reológicos no lineales. *Revista Internacional para Métodos Numéricos para Cálculo y diseño en Ingeniería* Vol. 20, 4, 355-374.
(23) Marí, A. (1993). Pérdidas. Software for calculating composite sections with Step-by-Step analysis. Barcelona, Spain.
(24) Fédération Internationale du Béton (FIB) (2012). *Model Code 2010-final draft*, Vol.1, Bulletin 65, and Vol.2, Bulletin 66.
(25) Statik v8 Frame Structures (2018). Cubus AG. Engineering Software. Zurich, Switzerland.